

Small Animal Model of Osteochondritis Dissecans

A Thesis
Presented to
The Academic Faculty

by

Destiny August Cobb

In Partial Fulfillment
of the Requirements for the Degree
Bachelor of Science in the
School of Wallace H. Coulter Department of Biomedical Engineering

Georgia Institute of Technology
May 2016

Small Animal Model of Osteochondritis Dissecans

Approved by:



Dr. Robert Guldberg, Advisor
School of Mechanical Engineering
Georgia Institute of Technology

Dr. Nick Willett
School of Biomedical Engineering
Georgia Institute of Technology

Date Approved:

Small Animal Model of Osteochondritis Dissecans

Approved by:

Dr. Robert Guldberg, Advisor
School of Mechanical Engineering
Georgia Institute of Technology



Digitally signed by Nick Willett
DN: cn=Nick Willett, o=Emory University,
ou, email=nick.willett@emory.edu, c=US
Date: 2016.04.26 10:27:49 -0400

Dr. Nick Willet
School of Biomedical Engineering
Georgia Institute of Technology

Date Approved: 4/26/16

[To the students of the Georgia Institute of Technology]

ACKNOWLEDGEMENTS

I would like to thank my PI and mentor, Dr. Robert Guldberg, as well as Giuliana Salazar-Noratto, for all they have taught me. I would also like to thank my mother and father, Patricia and Ashley Cobb, who have supported me from day one.

TABLE OF CONTENTS

	Page
ACKNOWLEDGEMENTS	iv.
LIST OF FIGURES	vi.
LIST OF SYMBOLS AND ABBREVIATIONS	vii.
ABSTRACT	viii.
<u>CHAPTER</u>	
1 INTRODUCTION	1
2 LITERATURE REVIEW	3
3 METHODS AND MATERIALS	5
SURGICAL PROCEDURE	5
EPIC- μ CT	5
HISTOLOGY	6
HUMAN BIOPSY SAMPLES	6
4 RESULTS	10
5 DISCUSSION	12
6 ADDITIONAL INFORMATION	13
REFERENCES	14

LIST OF FIGURES

	Page
Figure 1: JOCD LESION	2
Figure 2: SURGICAL PROCEDURE	6
Figure 3: SURGICAL SET UP	7
Figure 4: μ CT IMAGES	8
Figure 5: HUMAN BIOPSY SAMPLE	9
Figure 6: HISTOLOGY	10
Figure 7: THICKNESS MAPS	11
Figure 8: ATTENUATION, THICKNESS, AND VOLUME	11
Figure 9: 4 TH PILOT STUDY SURGICAL PROCEDURE	12

LIST OF SYMBOLS AND ABBREVIATIONS

JOCD	Juvenile Osteochondritis Dissecans
EPIC- μ CT	Equilibrium Partitioning of an Ionic Contrast Agent Micro-Computed Tomography
MIA	Monosodium iodoacetate

ABSTRACT

Juvenile Osteochondritis Dissecans (JOCD) is a joint disorder that predominantly affects athletic children and adolescents. It is characterized by the formation of osteochondral loose bodies which cause pain and swelling in the affected area, limit the patient's activity level, and in some cases requires surgery to fix or remove loose bodies depending on the stage to which the disorder has progressed. There is interest in developing preclinical animal models of the disorder to be used as a tool for developing regenerative therapeutics for treating the disorder. The objective of this project is to develop a small animal model of JOCD using Lewis rats. The model is being developed through a series of pilot studies with iterative modifications made to the procedure.

The surgical procedure aims to mechanically and chemically induce an initial lesion just below that subchondral bone, which would have a secondary effect on the overlaying cartilage over time. By drilling into the left medial femoral condyle, we are to create a 1 mm deep and 1mm wide defect. The right leg serves as the contralateral control. Pilot studies have relied on an injection of various doses of monosodium iodoacetate (MIA, in saline), a glycolytic inhibitor, into the cauterized drilled defect to induce the initial necrosis. The current procedure is being modified to create a thermal insult. 3 weeks post-surgery, the animals are euthanized and the morphology and integrity of the articular cartilage, including the thickness, volume, and attenuation, of both the left and right femurs are examined using EPIC- μ CT. This is followed by histological analysis. Additionally, diseased and healthy human biopsy cores provided by Children's Healthcare of Atlanta are being analyzed in a similar manner to provide a standard by which the model can be compared and its efficacy evaluated.

CHAPTER 1

INTRODUCTION

Juvenile Osteochondritis Dissecans (JOCD) is a joint disorder characterized by lesions in subchondral bone and overlying cartilage, the progression of which leads to osteochondral loose bodies⁵, as seen in Figure 1. Onset usually occurs during adolescence and is especially seen among athletes⁵. Though the cause of JOCD is not precisely known, a combination of trauma, ischemia, and genetic predisposition have been suggested⁵. Because knowledge of the etiology and progression of the disorder is limited, so too are the treatment options available. Current clinical treatment includes restricting physical activity and surgery to fix or remove loose bodies in the case of the advanced stages of the disorder¹.

Current research on JOCD primarily concern surgical procedure for treatment or relies on case studies, which are limited. While there have been suggestions of a variety of causes, the exact etiology and characteristics of progression on the cellular level remain unknown despite the disorder first being described over a century ago¹. The problem is further made complex by the likelihood of a combinatorial etiology.

The main methods of investigation and diagnosis in humans include imaging techniques such as MRI and CT scanning and arthroscopic procedures. Animal research, including genomic, imaging, and histological analysis, has been conducted on the disorder, especially in horses, dogs, and pigs due to the fact that juvenile osteochondritis dissecans naturally occurs in these animals². In a canine model proposed by Adam et al. in 1991, loose bodies were created surgically using a ceramic chisel³. Small animal models of JOCD are limited. A rabbit model was recently proposed by Lyon et al. in 2012 which consists of using a biopsy punch to create a loose body⁴.

This project endeavors to both further characterize the disorder and develop a small pre-clinical animal model in Lewis rats of JOCD of the knee. The knee and more specifically the posterolateral face of the medial femoral condyle has been selected as the defect site because it is the most common location for a JOCD lesion to form⁵. A small animal model is beneficial as compared to a large animal model because of the lower cost of acquiring and housing smaller animals and the fact that small animals progress in age faster, allowing studies to take place over shorter time spans. A small animal model of JOCD would be useful for proof of concept studies, which could then be translated to clinical models. In comparison with current preclinical animal models, this model instead uses both a mechanical and chemical methods of inducing a lesion, creating the lesion from below the subchondral bone, which matches more closely to current knowledge of how lesions form in humans. A long term aim is to pave way for new treatment options featuring personalized medicine based on genomic information and μ CT imaging. However, the genomic portion of this project is not covered in this proposal. This model

can serve as a platform for future studies testing new regenerative therapeutics and developing better treatment options for patients.

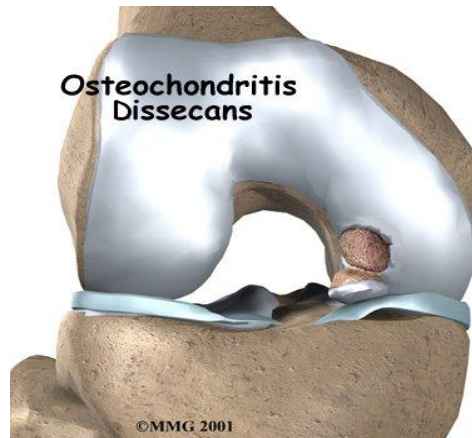


Figure 1. In JOCD, an initial lesion progressively damages the cartilage and subchondral bone, resulting in the separation of an osteochondral fragment⁶.

CHAPTER 2

LITERATURE REVIEW

The development and use of small animal models are often required for understanding and creating novel treatment methods for diseases. In particular, by providing proof of concept data, rodent models are a cost effective means of performing necessary intermediate studies between *in vitro* studies and large animal preclinical studies of cartilage regeneration. There is a plethora of emerging *in vitro* studies for potential methods of healing osteochondral lesions. While the occurrence of osteochondritis dissecans in large animals such as dogs and horses is well studied, the only small animal model currently existing is currently a rabbit model of JOCD³.

Common methods of inducing defects and creating cartilage loss in animal models include direct injury and injection of cytotoxic solutions into the joint space⁷. The former appears to be more common in creating osteochondral fragments. In 1991 Adam et al. published a study on the stability of osteochondral fragments of the femoral condyle of dogs.³ Their method used a ceramic chisel to chip away a fragment of the subchondral bone and overlying cartilage in varying ways to create different types of defects³. Similar methods of directly fracturing or fragmenting the condyle have been used in studies of JOCD using smaller animals such as rabbits³. Most notably, in 2013 Lyon et al. proposed a lapine model of JOCD for a pilot study on the healing potential of extracorporeal shock wave therapy on JOCD lesions⁴. The method of inducing a defect involved using a biopsy punch to extract a 4-mm wide and by 2-mm deep osteochondral fragment from the medial femoral condylar region of the knee⁴. In a similar manner a pilot study from Pfeifer et al. mimicked osteochondral lesions in Yucatan minipigs by placing a synthetic matrix between an extracted piece and the joint and then suturing the piece back into place.¹¹ However, this model only replicates stage 3 of JOCD, when the fragment is still partially attached, whereas the model being developed attempts to replicate the progression through each stage of the disorder.

The shortcoming of models of cartilage defects that use a direct method of mechanically creating a lesion is that isolated removal of an osteochondral piece likely behaves and responds to treatment in a fundamentally different way than that of fragment that develops over time from below the cartilage surface, as in JOCD. If a lesion can be induced through surgical methods beyond the simple removal of a piece of osteochondral tissue, the model may more accurately reflect the actual progression of JOCD and thus provide a better platform for testing the efficacy of emerging therapies.

While there have been several animal studies of JOCD utilizing rabbits, a rodent model would have similar limitations and advantages to rabbits. Namely, they are both considered small animals whose joint size and thin cartilage do not allow the creation of defects with dimensions comparable to that of in humans. Both are cheap and easy to

house and show some evidence of potential for spontaneous healing that would not occur in humans without treatment⁷. However, this is a non-issue in this instance as some cases of JOCD show spontaneous healing. This is due to its incidence in children and adolescents whose epiphyseal growth plate have not yet closed, creating greater intrinsic healing potential⁵. While the use of small animals limits direct translational value due to their small joint size and thin cartilage, it serves as necessary tool for screening newly developed *in vitro* therapeutic methods.

The purpose of this study is to establish a preclinical small animal model of JOCD in Lewis rats to serve as a platform for testing techniques for cartilage regeneration and repair. The model aims to create an initial necrotic lesion in an area just below the subchondral bone which would cause secondary effects to the articular cartilage similar to that seen in JOCD. To induce a lesion from below the articular cartilage, both mechanical and chemical methods are being used in the procedure. Mechanically, a defect is created in the joint by drilling 1 mm into the medial femoral condyle using a 1 mm surgical drill bit. Monosodium iodoacetate (MIA) is then injected into the created defect, allowing the solution to pool in the space beneath that articular cartilage. MIA has been shown to cause necrosis of osteochondral tissue⁹. Cauterization and obstruction of the defect using bone wax are used to staunch bleeding and ensure the retention of the MIA. In addition, techniques such as inducing a thermal insult using liquid nitrogen and inducing ischemia by ligating blood vessels are being explored.

In order to characterize cartilage morphology and integrity following the surgery, EPIC- μ CT (equilibrium partitioning of an ionic contrast agent) is being used to acquire data about the thickness, volume, and attenuation, a measure of proteoglycan content, of the articular cartilage rather than by gross analysis by visual inspection and use of grading system^{2,9}. If this model is proven successful in creating an initial lesion that progresses in a similar manner as JOCD, the model can be used as a critical stepping stone for the addition of new techniques to the currently highly limited repertoire of JOCD treatment.

CHAPTER 3

METHODS AND MATERIALS

Surgical procedure by monosodium iodoacetate (MIA) injection. Lewis rats of matched weight (275-300 mg) are operated on in order to induce clinical symptoms of JOCD. An opening of 1mm width and depth is drilled into the area just below the subchondral bone of the left femoral medial condyle. The opening is then cauterized to stop bleeding and covered in bone wax. 5 μ l of MIA (in saline) is surgically injected into the opening. For the sham surgery an identical procedure is done except only saline is injected. This is in order to differentiate between the effects of the drilling from the effects of the MIA. The right unoperated leg serves as the contralateral control. Three weeks after surgery the animals are sacrificed, and both the left and right legs are fixed in formalin before the femurs are dissected out and prepared for data collection.

EPIC- μ CT (equilibrium partitioning of an ionic contrast agent). The morphology and integrity of the articular cartilage of both the left and right femurs are found using EPIC- μ CT, a technique developed by the Guldberg Lab.¹² This method allows for analysis of the tomographic reconstruction of both bone and cartilage and subsequent analysis of the morphology of cartilage which would otherwise be difficult to detect. This is accomplished by utilizing an ionic contrast agent, hexabrix (30% by volume in PBS), in which samples are incubated at 37°C for 30 minutes to allow the hexabrix to diffuse into the tissue to equilibration. The contrast agent allows the differences in attenuation between soft and hard tissues to be visualized and proteoglycan content in cartilage to be detected and compared. The head of the femur of each sample is then scanned. Afterward, the sample is incubated in PBS at 37°C for 30 minutes to allow the hexabrix to diffuse out of the sample. The scanned images are then rotated to produce sagittal sections. The slices of the medial condyle are selected and the articular cartilage semi-automatically contoured. An evaluation is run that allows comparison of cartilage thickness, volume, and attenuation between the affected and unaffected leg, providing information about the efficacy of the JOCD model. Images of the scanned femurs with the contoured cartilage can be seen in Figure 4.

Histological analysis. After scanning is complete, the samples undergo paraffin embedding. Once embedded, the paraffin blocks are sliced to produce sagittal sections of the femoral head which are mounted on glass slides. DAPI, Hematoxylin and Eosin, and Safranin-O staining are carried out in order to produce qualitative data about the effects of the surgery. DAPI shows cell death, while H&E and Safranin-O show morphology and integrity of the tissue, specifically of the cartilage. Visualization of joint tissues allows the presence or absence of osteocytes around the necrotic lesion to be determined, absence of which is indicative of cell death.

Analysis of human biopsy samples. 4 human biopsy samples, one of which is pictured in Figure 5, of a JOCD patient were obtained from Children's Healthcare of Atlanta and were analyzed using the EPIC- μ CT and histological techniques listed above. The equilibration time of hexabrix diffusion into the human samples was found by incubating the samples in the 30% hexabrix solution at various time points, ranging from 30 minutes to 48 hours. The equilibration time was determined to be 12 hours. A new method of contouring the human cartilage was iteratively developed in order to produce the most accurate measurements of attenuation. Data from the human samples serves as an indicator of features of disease progression. 4 additional samples have since been obtained and are currently undergoing analysis.



Figure 2. Surgical procedure for the 3rd pilot study

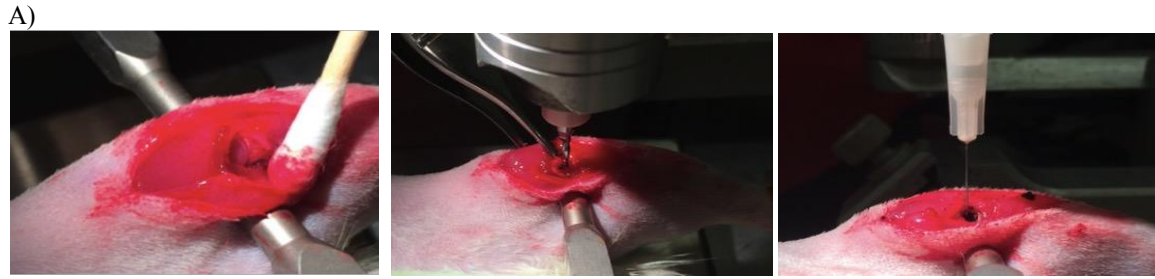
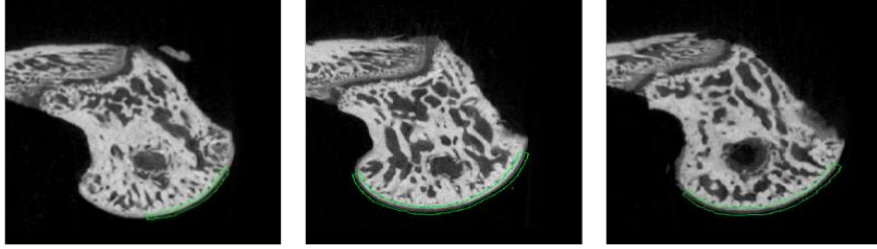


Figure 3. A. Stages of the surgical procedure. The ear bars are set up on either side of the knee, the drill and then syringe are positioned normal to the medial side of the condyle, and the MIA is injected into the drill hole. **B.** Stereotaxic frame and cauterizer set-up.

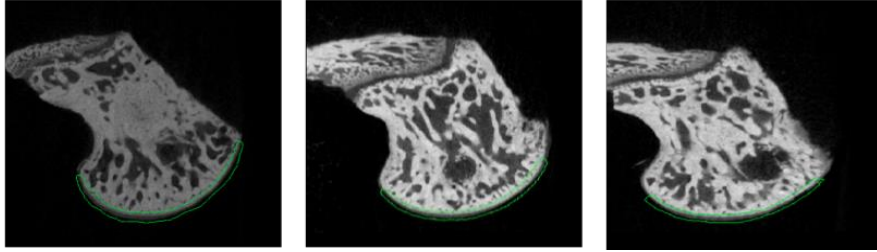
Though the stereotaxic instrument is typically used in neurosurgery, its use has been modified so that the knee is securely positioned between the ear bars, allowing continuous, stable access to the exposed medial side of the femoral condyle. The drill and syringe used to inject the MIA can then be attached to the frame and manipulated to move in 3 orthogonal planes of motion via dials, allowing precise positioning.

A)

OCD Group: 2 mg/50 ul



Sham Group



B)

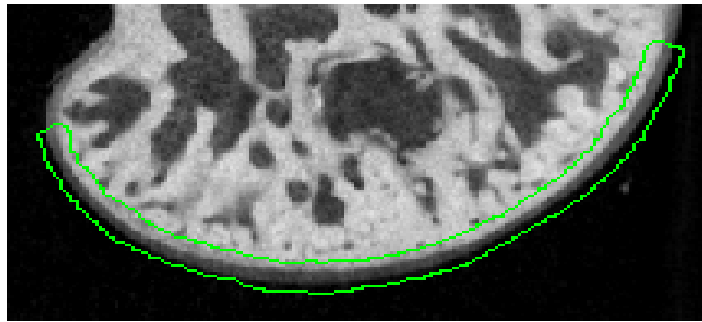


Figure 4. A. μ CT images of sagittal sections of the left femoral heads of both the OCD and the Sham group. **B.** Closer view of the cartilage of one of the OCD samples. The articular cartilage is circled in green. To standardize the contouring method, only fully defined cartilage overlying fully developed subchondral bone was selected. The black circular spot adjacent to the cartilage is the drill hole, which was spatially consistently across samples.

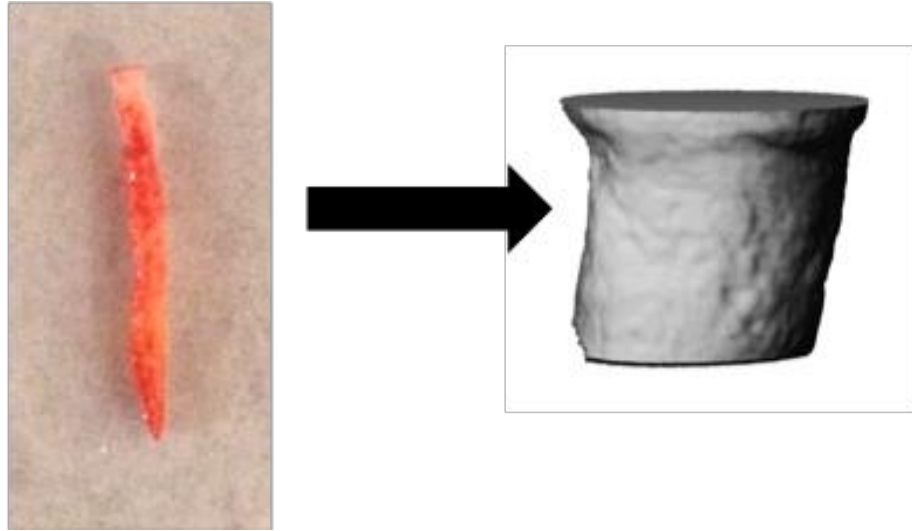


Figure 5. A JOCD human biopsy sample of the subchondral bone and articular cartilage (left) and the 3D μ CT reconstructed image of the articular cartilage generated after scanning, contouring, and evaluation (right).

CHAPTER 4

RESULTS

There has been some evidence of necrosis around the created defect, but no consistency across samples (Figure 6). Additionally, it was found that the bone was remodeling and healing around the drill area in all stains. The expected result of the JOCD samples is an increased attenuation which would indicate lowered proteoglycan due to cartilage degradation content to then be confirmed histologically. Cartilage attenuation is a quantitative measurement that is inversely proportional to the amount of proteoglycan in the cartilage. In this pilot study, no statistical difference in attenuation, average thickness, or volume was found between the control and JOCD samples (Figure 8). The cartilage of the JOCD joints appeared thinner than the contralateral controls (Figure 7, 8). Additionally, attenuation of the affected joints was greater, potentially indicating a lower proteoglycan content and thus more degradation than the controls (Figure 8).

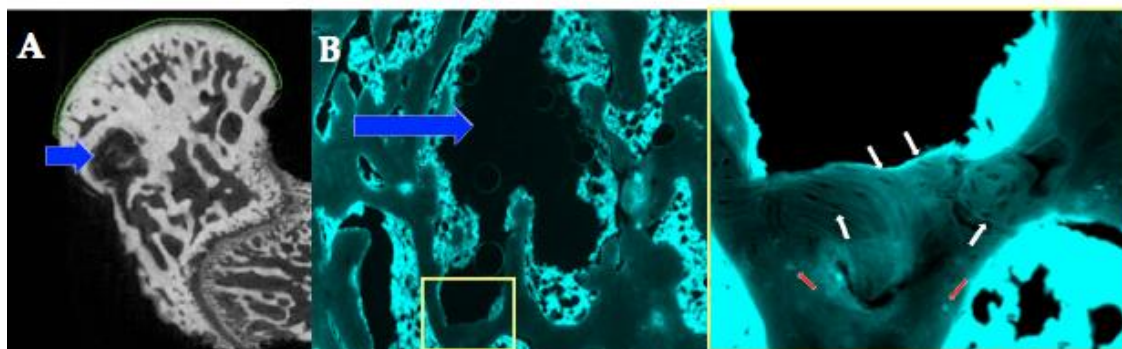


Figure 6. **A.** Sagittal view of medial femoral condyle shows the drill hole (blue arrow). **B.** Viability of tissue cells in the medial femoral condyle. The blue arrow points at the drill hole. The yellow box shows 20x magnification of the drill hole. White arrows point at lacunae empty of osteocytes indicative of bone death, while red arrows point at cell nuclei.

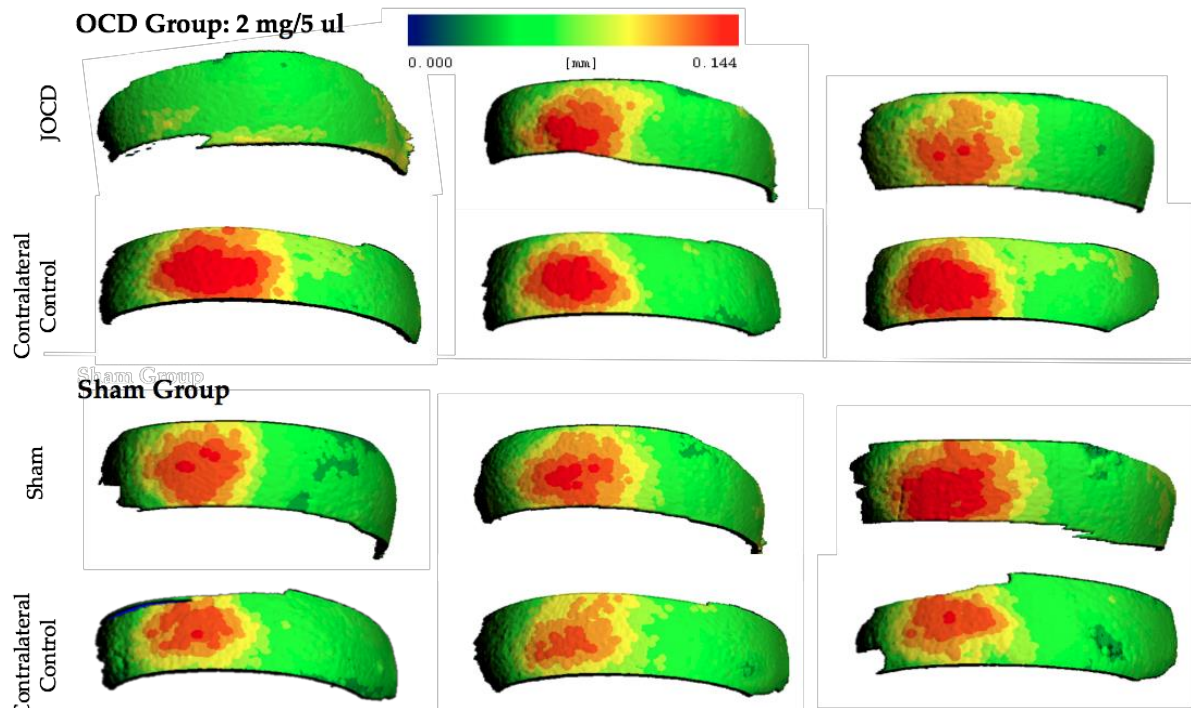


Figure 7. Thickness maps of the medial articular cartilage of the JOCD leg and the contralateral control for both the MIA and Sham groups.

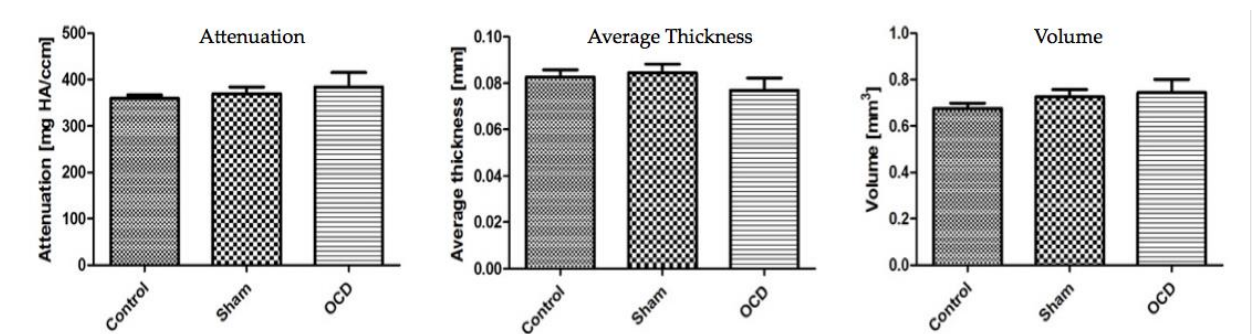


Figure 8. Attenuation (left), average thickness (center), and volume (right) of the control, sham, and JOCD groups.

CHAPTER 5

DISCUSSION

The results for the 3rd pilot study did not match that of the expected results. Over the course of 3 pilot studies, the procedure has been modified to improve upon the previous studies' results. The surgical procedure has evolved and been troubleshooted with the aim of standardizing the drill hole size and placement and the method of injection of MIA to prevent back flow and retain the solution within the opening, as well as finding the optimal concentration of MIA and a surgical set up that utilizes the stereotaxic frame to allow secure placement of the leg and precise drilling and injection, ensuring consistency between animals. Though the results of the EPIC μ CT analysis proved to be insignificant, the histological analysis did show cell death, meaning the parameters of the procedure may need to be adjusted.

Areas for alteration in the 4th pilot study include foregoing the use of MIA and instead using ligation of blood vessels to induce ischemia and stream liquid nitrogen to create a thermal insult the tissue on the medial side of the femoral condyle. These alterations are based on a paper by Consemius et al. in which a model of femoral head osteonecrosis was developed using a surgical procedure of vessel ligation and creating cryogenic insults¹⁰. The procedure for the 4th pilot study is shown in Figure 9.

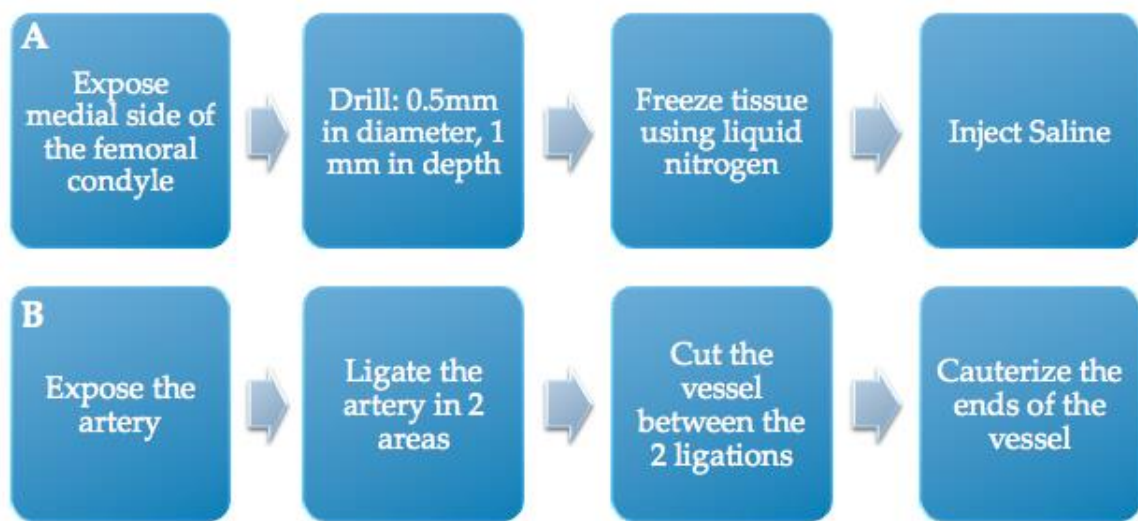


Figure 9. Surgical procedure for the 4th pilot study. Includes the use of **A.** cryosurgery (5 freeze/thaw cycles) and **B.** ligation of blood vessels.

CHAPTER 6

ADDITIONAL INFORMATION

This work was supported by a seed grant from the Children's Healthcare of Atlanta Center for Pediatric Innovation. The authors would also like to acknowledge the National Science Foundation Graduate Research Fellowship Program and the Petite Scholars Undergraduate Research Program.

This research has been presented in poster format at the 2014 Petite Scholars Poster Session, the TERMIS-AM 2014 conference, and the UROP 2015 Spring Symposium. This project has also been presented in an oral presentation at the Spring 2015 Undergraduate Research Kaleidoscope.

REFERENCES

1. Edmonds, E. W., & Polousky, J. (2013). A review of knowledge in osteochondritis dissecans: 123 years of minimal evolution from König to the ROCK study group. *Clinical Orthopaedics and Related Research*, 471(4), 1118–26. doi:10.1007/s11999-012-2290-y
2. Strömberg, B., & Rejnö, S. (1977). Osteochondrosis in the horse. I. A clinical and radiologic investigation of osteochondritis dissecans of the knee and hock joint. *Acta radiologica. Supplementum*, 358, 139-152.
3. Adam, G., Biihne, M., Prescher, A., Giinther, R. W., Nolte-ernsting, C., & Bohndorf, K. (1991). Skeletal Radiology Stability of osteochondral fragments of the femoral condyle : magnetic resonance imaging with histopathologic correlation. *Skeletal Radiology*, 601–606.
4. Lyon, R., Liu, X. C., Kubin, M., & Schwab, J. (2013). Does extracorporeal shock wave therapy enhance healing of osteochondritis dissecans of the rabbit knee?: a pilot study. *Clinical Orthopaedics and Related Research*, 471(4), 1159–65. doi:10.1007/s11999-012-2410-8
5. Green, J. (2012). Osteochondritis dissecans of the knee. *Journal of Bone & Joint Surgery, British Volume*, 47(5), 553–562. Retrieved from <http://www.bjj.boneandjoint.org.uk/content/48-B/1/82.short>
6. Orthopod. Osteochondritis Dissecans of the Knee: A patient's Guide to Osteochondritis Dissecans of the Knee. www.eorthopod.com/content/osteochondritis-dissecans-knee
7. Chu, C. R., Szczodry, M., & Bruno, S. (2010). Animal models for cartilage regeneration and repair. *Tissue Engineering Part B: Reviews*, 16(1), 105-115.
8. Aichroth, P. (1971). Osteochondral Fractures and Their Relationship to Osteochondritis Dissecans of the Knee. An Experimental Study in Animals. *Journal of Bone & Joint Surgery, British Volume*, 53(3), 448-454.
9. Thote, T., Lin, A. S. P., Raji, Y., Moran, S., Stevens, H. Y., Hart, M., ... & Willett, N. J. (2013). Localized 3D analysis of cartilage composition and morphology in small animal models of joint degeneration. *Osteoarthritis and Cartilage*, 21(8), 1132-1141.

10. Conzemius, M. G., Brown, T. D., Zhang, Y., & Robinson, R. A. (2002). A new animal model of femoral head osteonecrosis: one that progresses to human-like mechanical failure. *Journal of Orthopaedic Research*, 20(2), 303-309.
11. Pfeifer, C. G., Kinsella, S. D., Milby, A. H., Fisher, M. B., Belkin, N. S., Mauck, R. L., & Carey, J. L. (2015). Development of a Large Animal Model of Osteochondritis Dissecans of the Knee A Pilot Study. *Orthopaedic Journal of Sports Medicine*, 3(2), 2325967115570019.
12. Lin, A. S., Salazar-Noratto, G. E., & Guldberg, R. E. (2015). EPIC- μ CT Imaging of Articular Cartilage. In *Osteoporosis and Osteoarthritis* (pp. 131-140). Springer New York.